Solidification of infiltrated metal matrix composites

M. C. FLEMINGS, A. MORTENSEN and J. A. CORNIE, Department of Materials Science and Engineering, Massachusetts Institute of Technology, Cambridge, Massachusetts, U.S.A.

Abstract

This paper describes one portion of a broad continuing program at Massachusetts Institute of Technology on metal matrix composites. It deals with solidification of fibrous composites during and after infiltration. The fibers influence solidification in important ways by restricting the maximum size to which a dendrite arm can grow by "ripening". More remarkably, the dendritic structure in composites is completely eliminated at longer solidification times, as a result of "coalescence" and of enhanced solid diffusion. The result is that substantially more homogeneous structures can be obtained in metal-matrix composites than in usual castings and ingots.

Riassunto

Solidificazione di compositi infiltrati a matrice metallica

Questa memoria descrive una parte di un vasto progetto in corso al Massachusetts Institute of Technology sui compositi a matrice metallica. Si tratta della solidificazione di compositi fibrosi durante e dopo l'infiltrazione. Le fibre influenzano la solidificazione in larga misura, restringendo la massima dimensione alla quale un ramo di dendrite può arrivare per "maturazione". Più notevole è il fatto che la struttura dendritica nei compositi è completamente eliminata con tempi più lunghi di solidificazione, come effetto della coalescenza e della maggiore diffusione solida. Il risultato è che sostanzialmente si possono ottenere strutture più omogenee nei compositi a matrice metallica che nei normali getti e lingotti.

Introduction

Over the past several decades, the Solidification and Casting Group of the Department of Materials Science and Engineering at MIT has been engaged in a series of fundamental studies relating to casting processes and properties. Some of the important processes studied and developed in the laboratory have included "premium quality" light alloy castings (1), lost foam casting ("Policasting") (2), and semi-solid forming ("Rheocasting") (3). In searching for new or improved foundry processes, extensive work has also been conducted in fundamental areas including fluidity, microsegregation, macrosegregation, directional solidification, rapid solidification, and solidification of undercooled alloys.

In the past several years, the group has been broadened in scope and leadership to include metal matrix composite materials, and its name has been changed to the "Solidification and Composite Materials Group". Current work on composite materials in the group covers a wide spectrum including infiltration, "compocasting", solidification of composites, interface science and interface tailoring, and properties of composites. In this paper we describe that portion of our current work at MIT on infiltrated metal-matrix composites that involves solidification processing.

Solidification during infiltration

In one common method of producing metal-matrix composite parts, a preform of fibers is placed in a mold cavity, and metal is then caused to flow within the interstices. If the metal wets the preform well, it may be "wicked" in with little or no external pressure applied. If, at the other extreme, the metal and fibers are completely non-wetting, then a pressure is required to force the metal in that is the order of:

$$P \approx 2\gamma/r \qquad (1)$$

where γ is metal surface energy and r is effective pore radius. For example, for aluminum covered with a thin oxide film, $\gamma \approx 1$ N/m and for an effective pore radius of 1 μm a pressure of 2 MPa is required to fill the preform. Most results reported to date suggest that the heat flow problem in filling a preform is made very simple because of the fine fiber size and relatively low filling speed. These factors result in local thermal equilibration

Fig. 1 - Schematic illustration of infiltration of a fibrous preform by a pure metal.

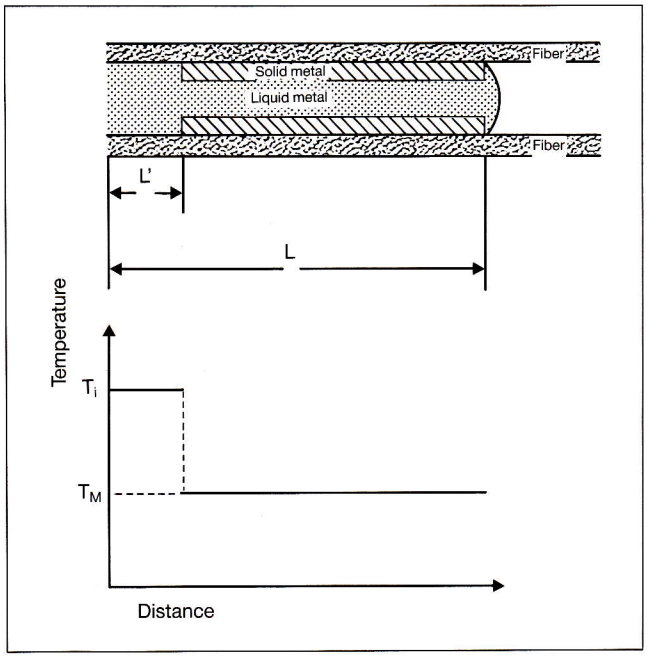

of the metal and the fiber at a very short distance behind the tip of the flowing liquid metal. Figure 1 shows this schematically for a pure metal initially at temperature T_i flowing into a fiber bundle which is initially at a temperature T_f, with T_f being less than the melting point of the metal, T_m. Superheat of the entering liquid metal is dissipated over a length L' and at a given time t during flow there is then a length L-L' which contains a uniform fraction solid, f_s^o which forms at the tip, at L. The region L' increases with time as the hot liquid remelts solid that originally formed. This problem is readily treated quantitatively by assuming negligible temperature differences in the direction transverse to flow and negligible heat transfer by conduction parallel to flow (4, 5, 6).
The problem becomes more complicated, and more interesting, when the case of alloy solidification is considered. This problem is the basis for current doctoral thesis work of L. Masur in our research group. Understanding the details of the infiltration problem is key to development of optimal techniques for producing complex infiltrated metal matrix composites that are free of macrosegregation and microporosity, and have minimum fiber-metal reaction.

Solidification after infiltration

It is possible to separate the problem of solidification during infiltration from that after infiltration by simply re-melting and then re-solidifying an infiltrated metal-matrix composite.
This was done in two recent doctoral theses in our group at MIT, both of which employed the model Al-4.5% Cu alloy (9, 10).
In the first of these studies, the metal alloy was pressure infiltrated into preforms of carbon/silicon carbide fibers, 140 μm diameter (AVCO SCS-2 fibers). Small cylindrical specimens of the infiltrated composites were then placed in a vertical Bridgeman furnace, Figure 2, and solidified at various controlled rates and gradients so that the local solidification time of portions of the samples solidified at steady state ranged from 4s to 940s. Most specimens were abruptly quenched at a given time during solidification to reveal the dendritic structure; an example is shown in Figure 3. Photomicrographs such as this show, in one sample, dendrite arms where "local solidification time" varied from a very low value near the dendrite tip (because it was quenched soon after solidification began) to the "steady state local solidification time" t_f for the rate and gradient employed (at the point that was just solid at the time of quenching).
The dendrite tips in samples such as that shown in

Fig. 2 - Bridgeman furnace for steady state solidification experiments.

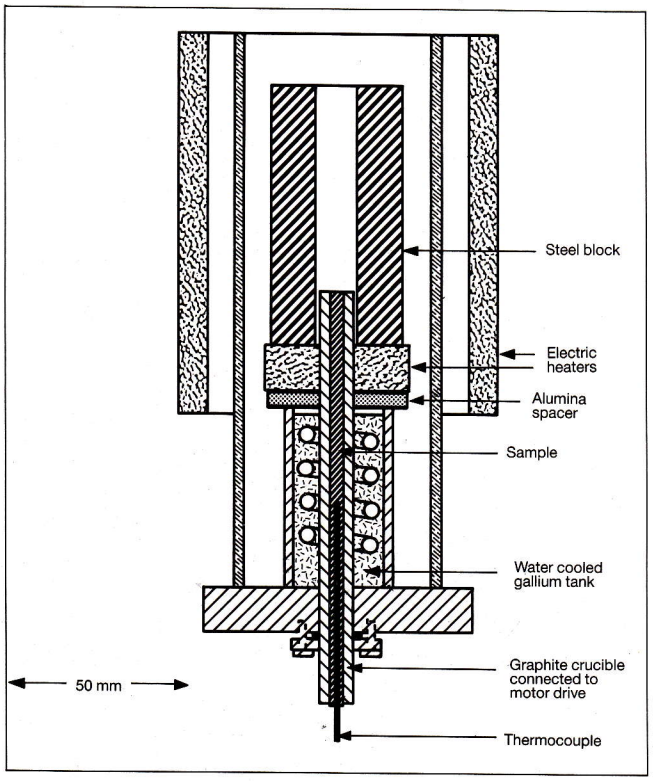

Fig. 3 - Dendrites, growing in a large interstice (right) and a small interstice (left). The dendrite in the center interstice intersects the plane of polish only near the bottom of the figure.

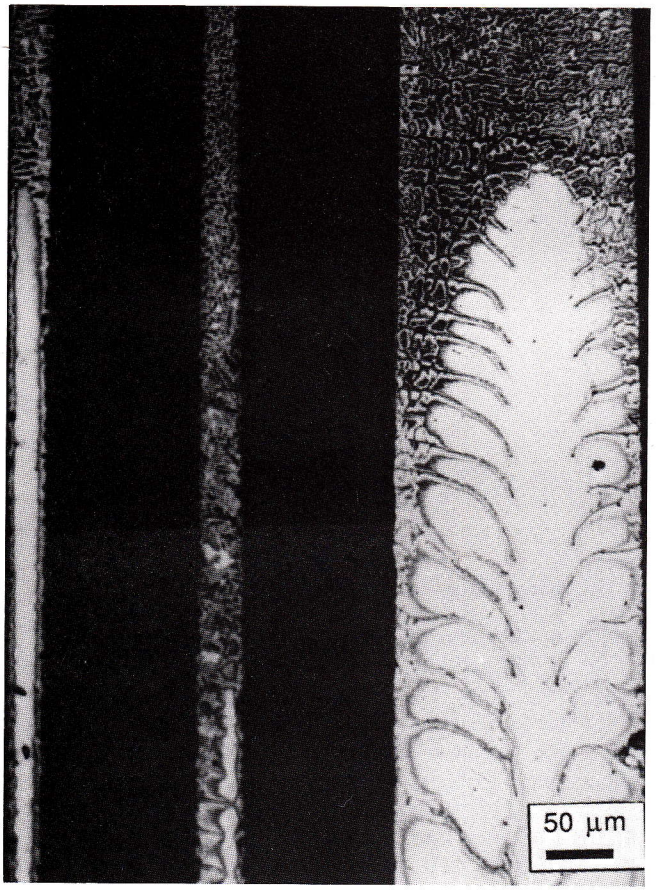

Figure 3 all grow at temperatures very near the liquidus, as they do in the unreinforced alloy. Behind the tips, secondary arms form in all interstices. The spacings between the arms can be measured as a function of time t spent in the liquid-solid region by simply measuring these spacings at increasing distance back from the tip. These spacings increase with increasing time in the liquid-solid region (local solidification time t). They do so as a result of coarsening, a surface tension driven phenomenon that reduces the total liquid/solid interfacial area. Coarsening is also observed in unreinforced castings, but it usually occurs more rapidly in the reinforced than in unreinforced castings. Results of measurements on a sample which had a steady state local solidification time of 268 seconds are shown in Figure 4. Data shown in this figure are for dendrite arms in the interstices between three closely spaced 140 micron fibers, while the straight line gives the standard $t^{1/3}$ relationship between dendrite arm spacing and local solidification time for the unreinforced alloy under steady state solidification.

Fig. 4 - Experimental points for secondary dendrite arm spacing versus local solidification time for a small interstice between three close packed SiC fibers 140 microns in diameter.
Steady state solidification time t_f for the sample was 268 seconds.

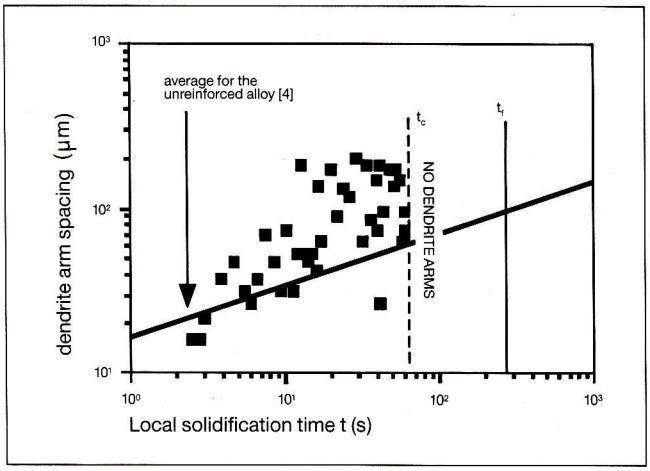

A remarkable phenomenon is seen in Figure 4, at a critical local solidification time of about 70 seconds, which is less than a third of the steady state solidification time t_f of this sample. Dendrite arms are no longer seen at all; they have totally disappeared during the solidification process. This is something that never occurs in usual castings and ingots, regardless of how slow cooling is.
In usual castings and ingots, secondary dendrite arms grow progressively during most of solidification by a process of coarsening that is termed "ripening". Small arms tend to re-melt while large ones grow. The driving force is surface energy, and mass transport is by diffusion through the liquid. This process has been studied by a large number of investigators, several of whom have developed quantitative treatments for the ripening process (11, 12). These treatments all give, in one form or another, the standard relationship of dendrite arm spacing to local solidification time, t_f, or to cooling rate, c:

$$d = At_f^{1/3} \quad (2)$$

$$d = B\,(c^{-1/3}) \quad (3)$$

The first of these relationships is plotted as the solid line of Figure 4. The process is shown schematically in Figure 5.

Fig. 5 - Ripening mechanisms for secondary dendrite arms.

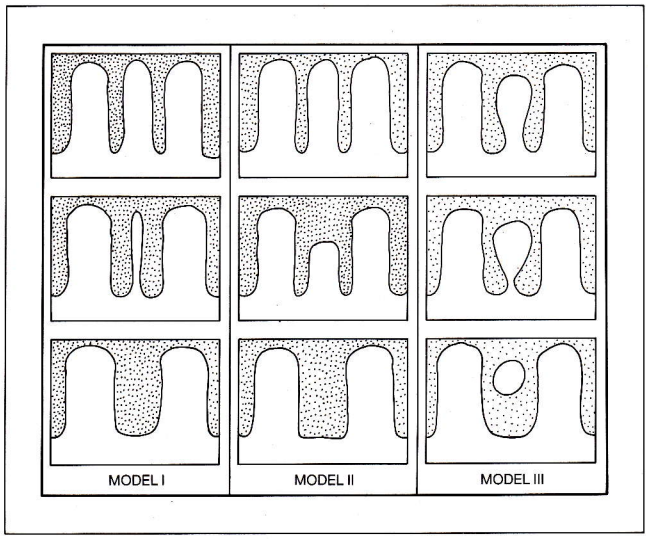

Toward the end of solidification at high volume fractions solid, a different coarsening method becomes operative; i.e. a different mechanism operates to reduce liquid-solid surface area of the solidifying alloy. That mechanism is "coalescence" whereby interdendritic regions "fill in" with solute, again with mass transport by diffusion through the liquid. In usual castings and ingots, this mechanism accounts for the "platelike" dendrite structures often seen, but it never results in elimination of the dendrite structure itself. The mechanism is shown schematically in Figure 6, and Figure 7A shows how the two mechanisms combine to produce solidification structures observed, for the case of directionally solidified castings and ingots.
In composites, the same two processes occur, but the essential difference is that the "ripening" shown schematically in Figure 5 can occur only until the secondary arms are of a size comparable to the interfiber spacing. Their further growth is then restricted by the fibers, and subsequent coarsening is

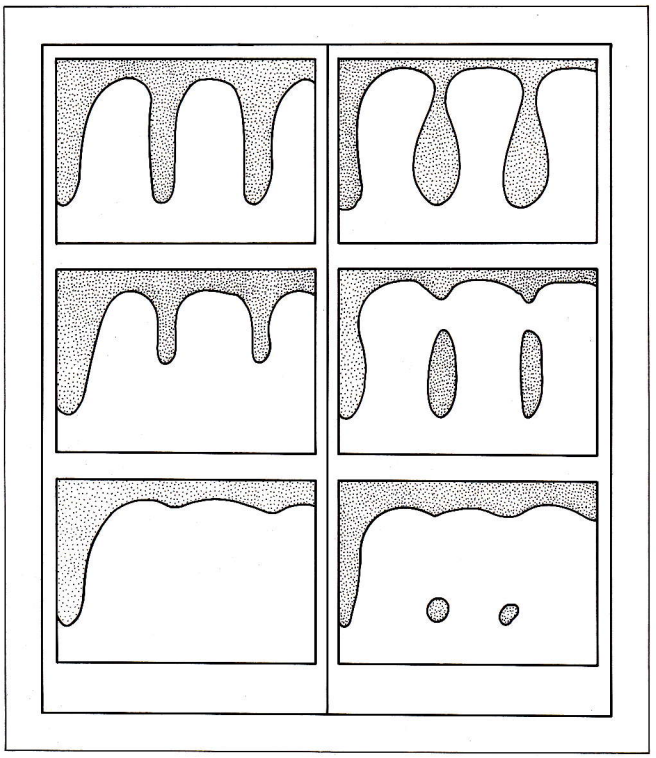

Fig. 6 - Coalescence mechanisms for secondary dendrite arms.

by coalescence. This coalescence then occurs much more rapidly than in usual castings and ingots, since the size scale of the structure is restricted by the fibers. Figure 7B shows how the process rapidly eliminates the short secondary dendrite arms in the composite during solidification. The ultimate result is the elimination of any observable dendritic structure at sufficiently long local solidification times.

Coalescence was further studied in doctoral thesis work of M. Gungor, in which the Al-4.5% Cu alloy was infiltrated into preforms of fine alumina fibers, 20 microns diameter (DuPont "FP" fibers). In these experiments, the infiltrated composites were re-melted, re-solidified at known cooling rates with very low temperature gradients, and then quenched at various times during solidification. Thus, the structure within a given sample was uniform throughout the sample, and greater statistical data could be obtained on dendrite arm spacing. Results are shown in Figure 8. Whether or not the dendrites actually disappear by coalescence in a given situation depends on cooling rate and fiber spacing. Here, for a fixed average fiber spacing, as the solidification time t_f increases (or conversely as the cooling rate decreases), the dendritic microstructure is eliminated. This process is evident in Figure 8. As the cooling rate decreases and, hence, the solidification time t_f increases, secondary dendrite arms become fewer and less well-defined. In a sample solidified in 750 seconds, the matrix has had time to "erase" nearly all dendrite arms, and the microstructure is thus essentially non-dendritic.

We have treated the foregoing coalescence problem quantitatively, and have obtained good agreement of theory with experiment in relating the critical time for disappearance of dendrites, t_c, with steady state solidification time, t_f, and with geometric parameters of the SiC reinforced Al-4.5 wt% Cu matrix composites (9). A comparison of theory with experiment is given in Figure 9.

In the alumina reinforced composites, the kinetics of dendrite arm coarsening were also accelerated by the

Fig. 7 - Schematic diagram of four stages during dendritic growth of Al-4.5wt%Cu alloy in a fiber-free alloy (left) and between fibers (right).

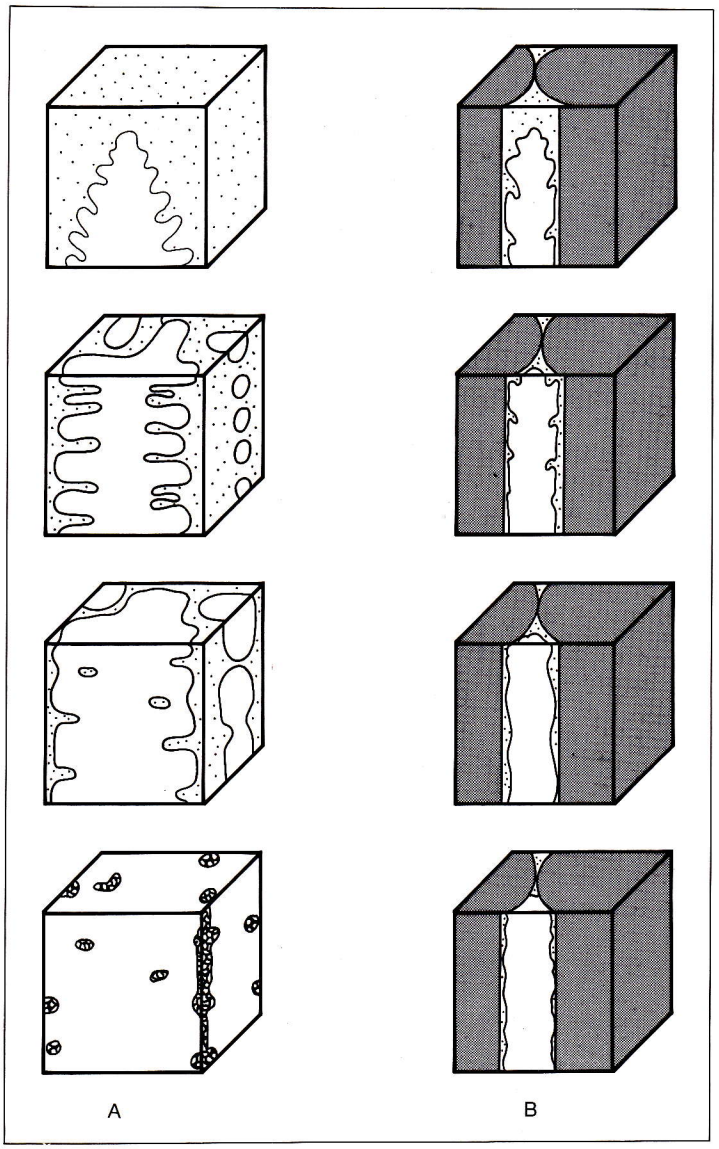

Fig. 8 - Microstructural evolution of Al-4.5wt%Cu reinforced with continuous alumina fibers 20 microns in diameter as the solidification time t_f varies from A) 1.3 s to B) 18s; C) 192s and D) 750s. It can be noted that the microstructure gradually becomes less dendritic as the solidification time increases.

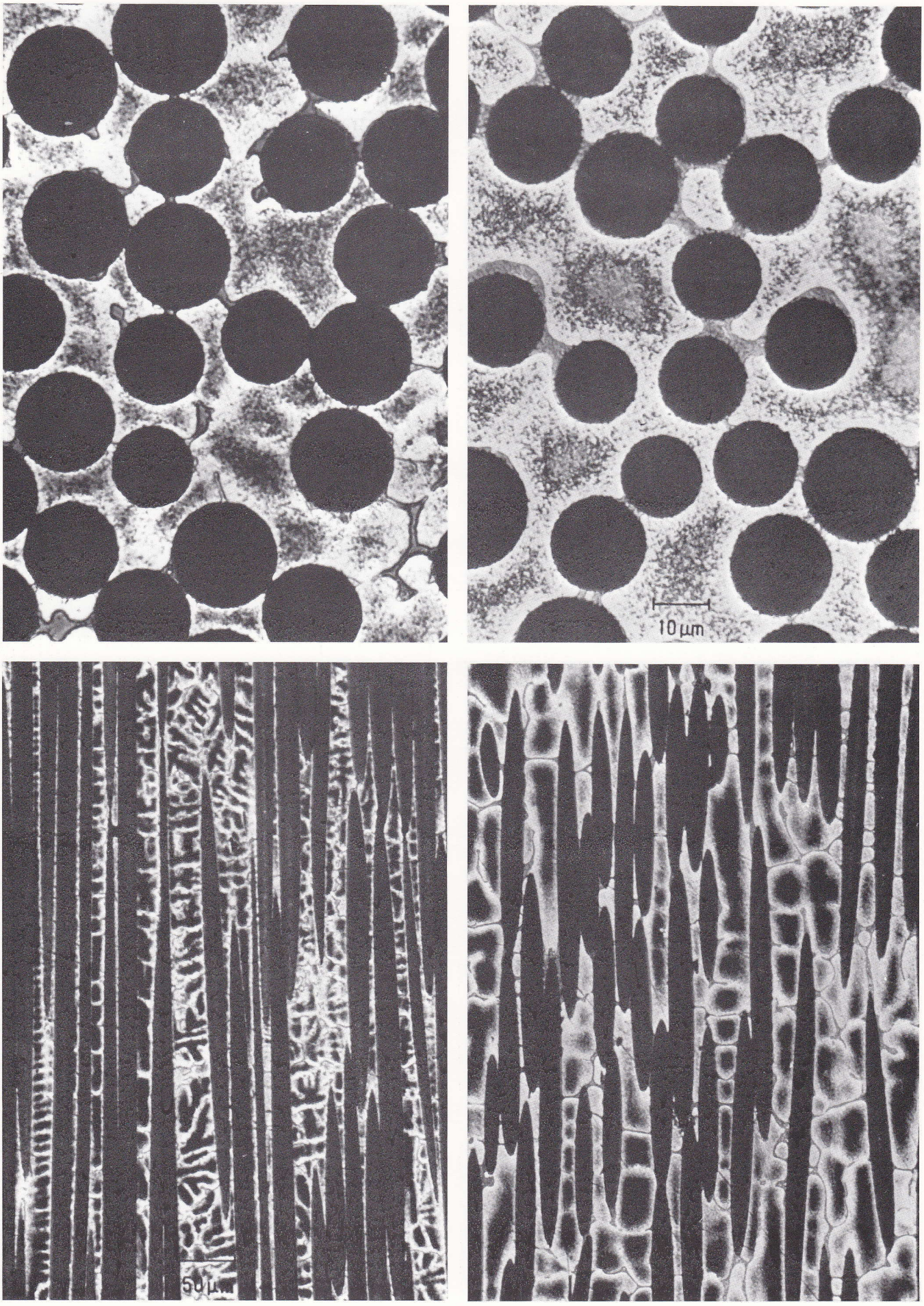

Fig. 8 - (continued)

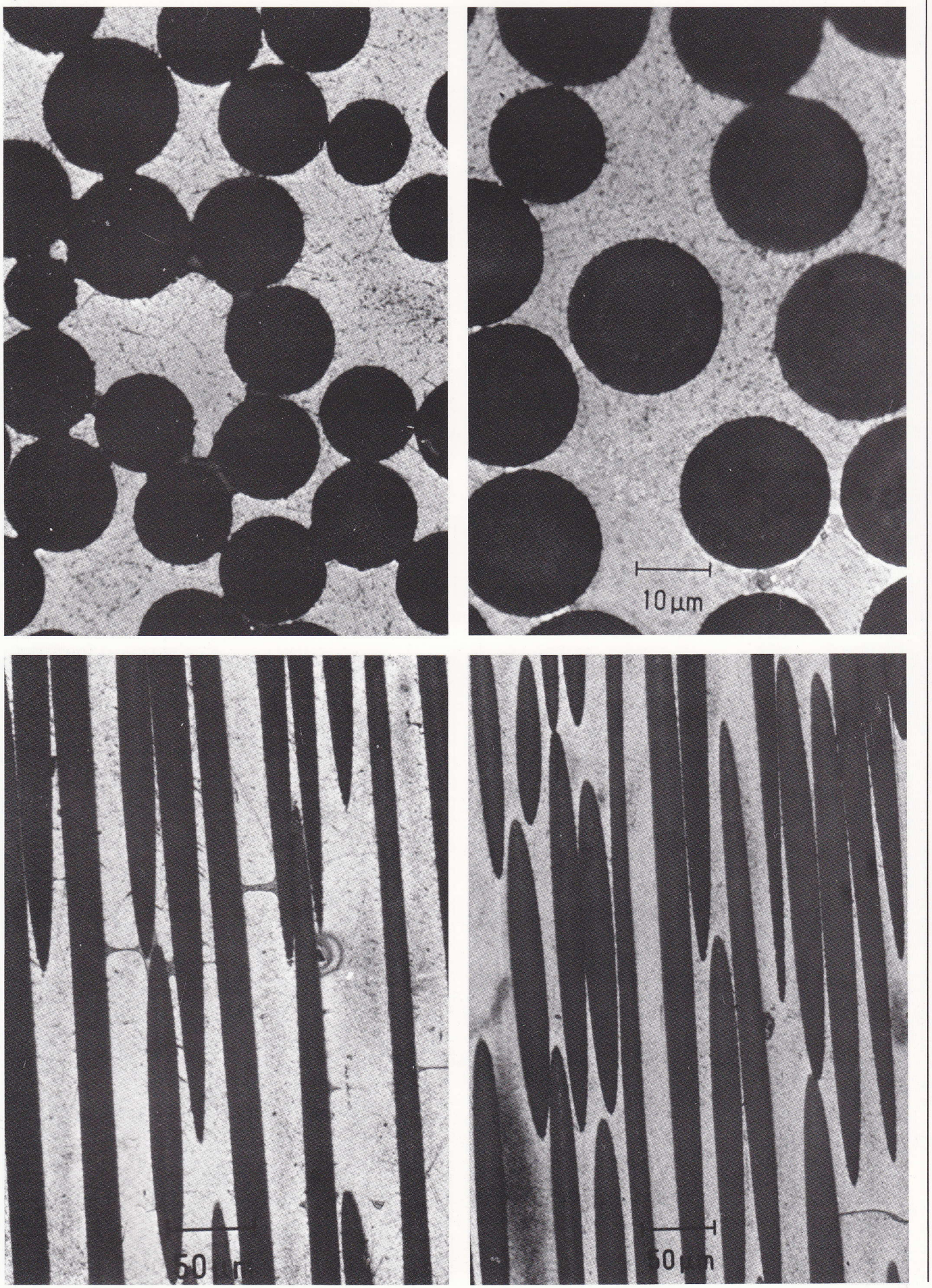

C D

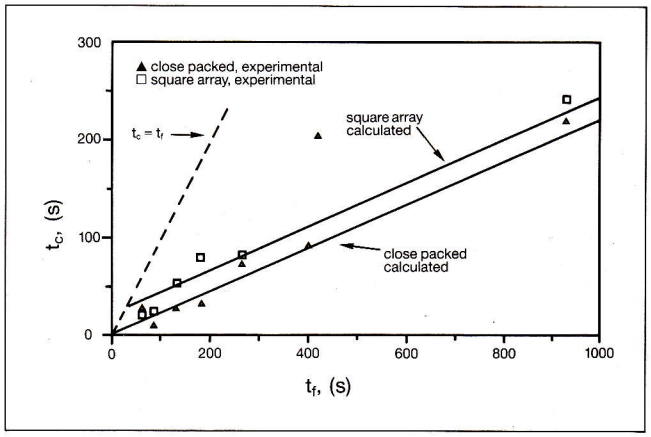

Fig. 9 - Comparison of measured and predicted time for complete coalescence of secondary dendrite arms in Al-4.5 wt%Cu reinforced with SiC fibers 140 microns in diameter. Experiments and calculations are for interstices between close packed fibers, and between touching fibers in a square array.

fibers (Figure 10). Instead of the usual relationship for castings:

$$\lambda_2 = 7.5\ t_f^{0.39} \qquad (4)$$

where λ_2 is the secondary dendrite arm spacing in microns, and t_f the solidification time in seconds (8). The following relationship holds for the composite:

$$\lambda_2 = 9.7\ t_f^{0.51} \qquad (5)$$

with only slight dependence on fiber volume fraction (Figure 10).

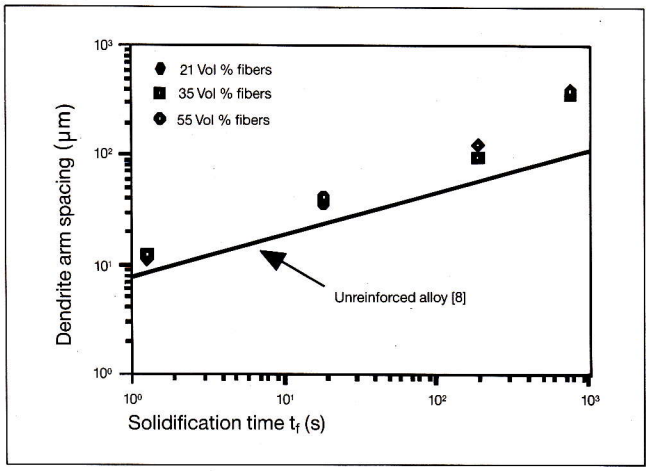

Fig. 10 - Secondary dendrite arm spacing versus solidification time t_f for usual castings and ingots (from reference [8]) and for Al-4.5wt%Cu reinforced with alumina fibers 20 μm in diameter.

Microsegregation

Coalescence modifies the morphology of the solidified matrix microstructure, but does not decrease "coring"

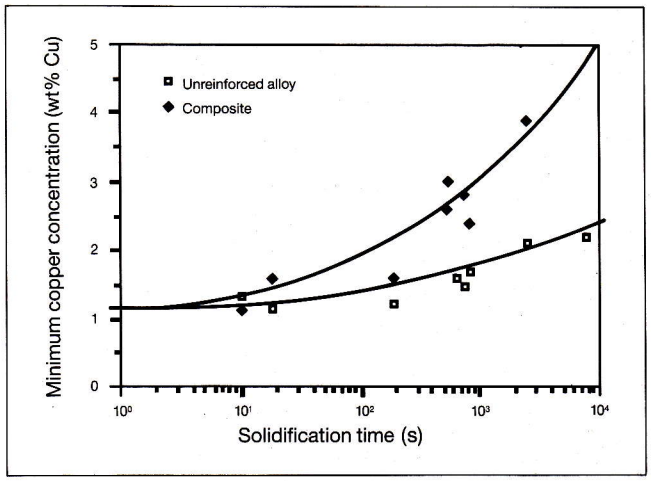

Fig. 11 - Minimum copper concentration in fiber-free Al-4.5 wt%Cu and Al-4.5wt%Cu reinforced with alumina fibers as a function of the solidification time t_f.

in the solid metal measured by minimum composition observed at the center of dendrites, nor does it result in full elimination of eutectic in the structure. These can be achieved only by diffusion in the solid during and after solidification. Homogeneity, as measured by these factors, is much greater in the composite than in usual castings and ingots, as shown by the data of Figure 11. At the longer solidification times, homogenization is virtually complete, with the minimum composition measured in the metal matrix approaching the maximum overall composition of 4.5% Cu. This result also follows directly from the restraint of the fibers on the dendrite size. The reduced dendrite spacing increases the critical dimensionless parameter for diffusion, Dt/d^2, where D is solid diffusion coefficient, t is time and d is dendrite arm spacing. Here, at the same diffusion time, t, the extent of diffusion is greater in the composite. This process was modeled for Al-4.5 wt% Cu reinforced with SiC fibers, and results from calculations agreed with experiment, indicating that solid state diffusion is indeed responsible for the observation.

Conclusion

Investigators in many laboratories throughout the world are studying metal-matrix composite materials, and engineering applications for these materials. Results of work presented herein show that control of solidification of such composites can produce matrices that are much more homogeneous than usual cast materials. Thus the designer is provided a new and potentially important tool for tailoring optimum properties in his composite.

REFERENCES

(1) Flemings, M.C., and H.F. Taylor. Premium quality light alloy castings. ***Aerospace Engineering,*** *(July 1962), 10-15.*

(2) Duca, A., M.C. Flemings, and H.F. Taylor. Art casting. ***Trans. A.F.S., 70*** *(1962), 60-61.*

(3) Spencer, D.B., R. Mehrabian, and M.C. Flemings. Rheological behavior of Sn-15% Pb in the crystallization range. ***Met. Trans., 3*** *(1972), 1925-1932.*

(4) Fukunaga, H., and K. Goda. ***Bulletin of the Japanese Society of Mechanical Engineering, 27*** *(June 1984), 1245.*

(5) Nagata, S., and K. Matsuda. ***Trans. Japanese Foundryman's Society, 2*** *(1983), 616.*

(6) ***Ibid., 3*** *(1984), 35.*

(7) Masur, L. Current research. MIT.

(8) Bardes, B.P., and M.C. Flemings. ***Trans. A.F.S., 74*** *(1966), 406.*

(9) Mortensen, A. Solidification of Al-4.5 wt% Cu in the presence of SiC fibers. Sc.D. Thesis, MIT, June 1986.

(10) Gungor, M. Solidification processing of Al-4.5% Cu/Al_2O_3 composites. Sc.D. Thesis, MIT, Sept. 1986.

(11) Kattamis, T.Z., J.M. Coughlin, and M.C. Flemings. Influencing of coarsening on dendrite arm spacing of aluminum-copper alloys. ***Trans. Met. Soc., AIME, 239*** *(1967), 1504-1511.*

(12) Young, K.P., and D.H. Kirkwood. ***Met. Trans., 6A*** *(1975), 197.*